How Does the Urea Dynamics Differ from Water Dynamics inside the Reverse Micelle?

ARTICLE *in* THE JOURNAL OF PHYSICAL CHEMISTRY A · SEPTEMBER 2011

Impact Factor: 2.69 · DOI: 10.1021/jp206069z · Source: PubMed

3 AUTHORS, INCLUDING:

Partha Hazra

Indian Institute of Science Education and Re…

52 PUBLICATIONS **997** CITATIONS

SEE PROFILE

THE JOURNAL OF PHYSICAL CHEMISTRY A

ARTICLE

pubs.acs.org/JPCA

How Does the Urea Dynamics Differ from Water Dynamics inside the Reverse Micelle?

Abhigyan Sengupta, Rahul V. Khade, and Partha Hazra*

Department of Chemistry, Indian Institute of Science Education and Research (IISER), Pune 411021, Maharashtra, India

ABSTRACT: In this study, the urea dynamics inside AOT reverse micelle (RM) has been monitored without intervention of water using time-resolved fluorescence techniques from the picosecond to nanosecond time regime. It has been observed that urea dynamics inside the reverse micelle is severely retarded compared to water RM due to the formation of highly networked urea cluster inside the RM. Time-resolved fluorescence anisotropy study also confirms the existence of a confined environment around the dye at higher concentrations of urea inside the reverse micelle. The dynamics of urea−water mixtures inside AOT reverse micelle has also been monitored with increasing urea concentration to get insight about the effect of urea on the overall solvation dynamics feature. It has been observed that with the increase in urea concentration, the overall dynamics becomes slower, and it infers the presence of few water or urea molecules, those strongly associated with surrounding urea and (or) water by hydrogen bonds.

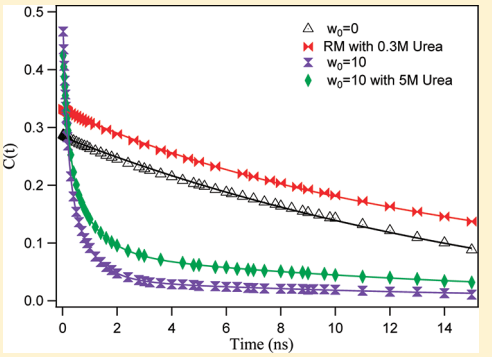

1. INTRODUCTION

For the past few decades, aqueous urea solution has been pervasively used as protein denaturant, which brought about burgeoning interest in the past and is still an attractive topic for present research. However, the mechanism of protein denaturation by urea is still a debatable topic. Two distinct mechanisms are offered regarding urea-induced denaturation of protein.[1−10] In one case, it is considered that urea wanes the hydrophobic interaction, and in other, it is proposed that urea weakens the intramolecular proteinous hydrogen bonds while directly binding to proteins.[1−10] Now an important question arises: at what extent is the hydrogen bond network of water perturbed by the addition of urea in water? To understand the properties of the urea−water system, a great deal of research has been carried out by using a variety of experimental and theoretical techniques. However, no common consensus has been reached among these studies. Some work suggests that urea breaks the water structure and is termed as a "structure breaker" or "chaotrope".[11,12] Others find urea to enhance the water structure, and so it can be termed as "structure maker" or "kosmotrope".[13,14] However, a number of recent studies also suggest a combination of both effects.[2,15,16]

Dielectric relaxations, NMR, and optical Kerr effect (OKE) techniques have been used to get dynamical information of water in urea−water solution.[17−19] Although dielectric relaxation and OKE techniques offer dynamical information on a picosecond time scale, these techniques monitor the dynamics of both urea and water in the solution and make it difficult to strike out urea response from the observed dynamics.[17,18] NMR study could selectively probe the water dynamics. However, it cannot distinguish water in the urea solvation shell from the bulk.[19] Very recently, infrared pump−probe spectroscopy has been employed to study the effect of urea on the structure and dynamics of water, and it was found that even at high concentrations of urea (8 M), the orientation dynamics of most of the water molecules are the same as in pure liquid water.[20] This infers that urea has negligible effect on the hydrogen bond dynamics of the water molecules.[20] However, a small fraction of the water molecules display orientational dynamics, which is more than six times slower than bulk water.[20] It was suggested that these water molecules are tightly associated with urea, forming a specific urea−water complex.[20] The short time dynamics of the water−urea mixture is also studied by molecular dynamics (MD) simulation, and the results indicate that the addition of urea leads to an overall isotropy and stiffening of the short time dynamics of both the species.[21] Both the experimental and simulation studies showed that diffusion of urea decreases with the increase in urea concentration in water.[22−24] Moreover, increasing urea concentration retards water diffusion.[22,23] Most of these studies have been focused to probe the dynamics of water in urea−water mixtures, so that it could predict whether water is strongly or loosely hydrogen-bonded in the presence of urea.[17−21] There are few reports where the dynamics of urea has been monitored as a function of urea concentration in water.[22−24] However, reports of urea dynamics without intervention of water are scarcely available. Considering the importance of urea in the protein denaturation process[1−10] as well as recent interest in urea as nonlinear optical material,[25,26] it would be worth to elucidate the dynamical feature of urea alone without intermediation of water. Experimentally, it is very difficult to monitor the dynamics of urea alone as urea has to be dissolved in water and in that case the observed dynamics will

Received: June 28, 2011
Revised: August 13, 2011
Published: August 29, 2011

dx.doi.org/10.1021/jp206069z | J. Phys. Chem. A 2011, 115, 10398–10407

Scheme 1. Structure of Coumarin-343 (C-343)

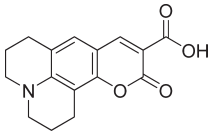

Coumarin-343

embrace the combinatorial effect of both water as well as urea. Recently, the solubilization property of urea in dry AOT reverse micelle (RM) has been investigated with the help of small angle neutron scattering (SANS) and FT-IR studies, and it is confirmed that urea is encapsulated in the micellar core as molecular clusters.[27,28] These studies pave a way to elucidate urea dynamics without intervention of water inside the reverse micelle.

In this work, we have investigated urea dynamics inside the RM as a function of urea concentration with the help of time-resolved Stokes shift method, and we believe that this is the first experimental attempt to unravel the dynamics of urea without intermediation of water. For comparison, water dynamics inside the RM has also been measured at various concentrations of water. Furthermore, we have studied urea−water mixture at various concentrations of urea inside the RM to estimate the effect of urea on overall dynamics. Here, Coumarin 343 (Scheme 1) has been chosen as a solvation probe because of it is extensive use in solvation dynamics studies.[29−31] Moreover, due to low solubility of Coumarin 343 (C-343) in hydrocarbon solvents, it prefers to reside at the RM interface or interior avoiding problems of partitioning between organic bulk solvents and RM and makes it possible to interpret the observed results without any ambiguity. We anticipate that our results give a comprehensive picture of urea dynamics with or without water, which might lead to the explanation of the protein-denaturing behavior of urea. Moreover, the new dynamic properties of urea inside the AOT-RM might take a major role for the fabrication of urea as a nonlinear optical material.

2. EXPERIMENTAL SECTION

C-343 was procured from Sigma Aldrich and used without further purification. Dye concentration was kept at 3×10^{-5} M for all the experiments. Dioctyl sulfosuccinate sodium salt (AOT, Sigma Aldrich, 98% pure) was dried under high vacuum for 24 h to eliminate the adsorbed water before use. *n*-Heptane (SRL, India, spectroscopic grade) was used as received. The AOT concentration was fixed at 0.38 M in all the RMs. RMs having three different concentrations of urea (0.046, 0.213, and 0.30 M) were prepared by adding precisely weighted solid urea to the AOT/*n*-heptane solution containing the probe molecule (C-343). The urea solubilization in AOT/*n*-heptane solutions was expedited by the ultrasounds. Each solution was sonicated for 1 h with an interval of 5 min and kept overnight in a thermostat having a temperature of 25 °C. The maximum amount of urea that can be dissolved in these solutions (expressed as [urea]/[AOT] = 0.96 at 25 °C) is equivalent to 0.3 M urea in AOT-RM.[27,28] This amount was practically independent of the AOT concentration and nature of apolar solvents used.[27,28]

The w_0 value for water RM is defined by the molar ratio of water to surfactant, w_0 = [water or urea]/[AOT]. Water RM solutions of various w_0 were prepared by the addition of an appropriate amount of water to the AOT/*n*-heptane system, and each of the solutions was equilibrated for several hours before use. Water RMs having different urea concentrations were prepared by adding aqueous solution of different urea concentration at a fixed w_0 (w_0 = 10).

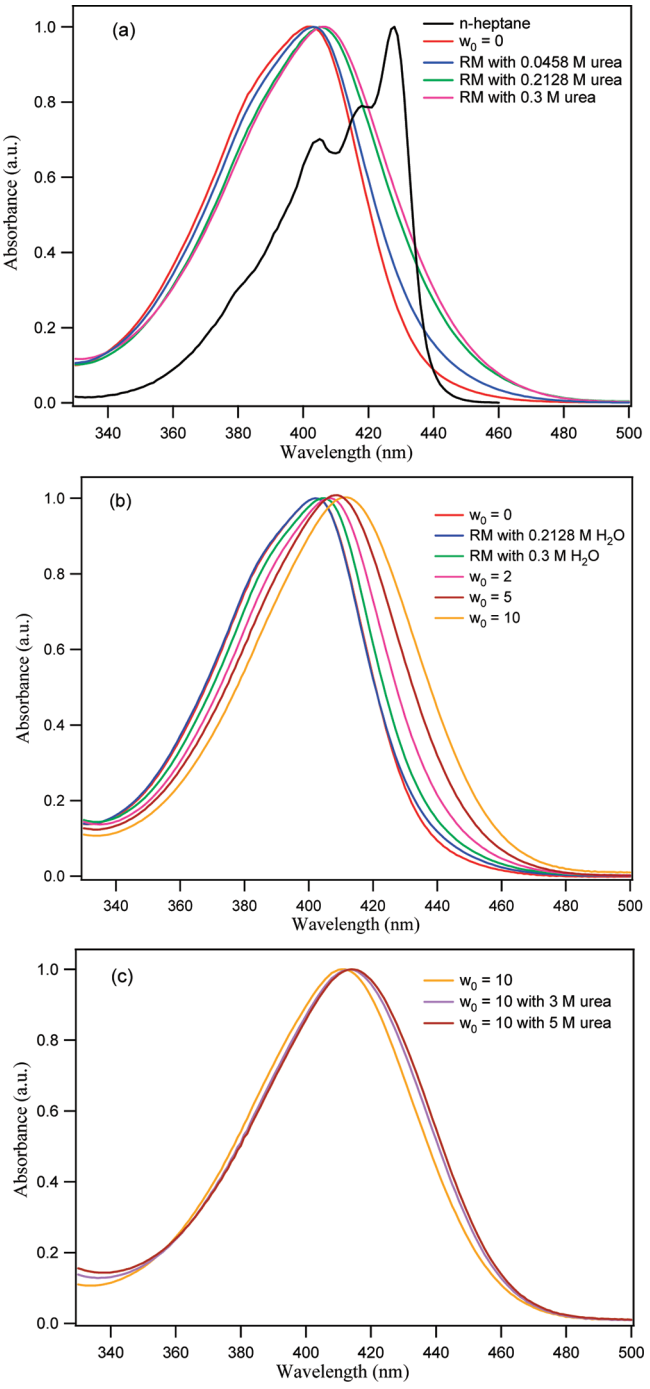

Figure 1. Absorption spectra of C-343 (a) in *n*-heptane and different concentrations of urea in AOT RM, (b) at different concentrations of water in AOT RM, and (c) at w_0 = 10 and two different concentrations of urea in RM at w_0 = 10.

Absorption spectra were recorded in an Evolution 300 UV−visible spectrophotometer (Thermo Fisher Scientific, U.S.), and Fluorolog-3 (Horiba Jobin Yvon, U.S.) was used to collect the fluorescence spectra. Fluorescence lifetime decays were collected by a time-correlated single photon counting (TCSPC)

Table 1. Absorption and Steady State Emission Maxima of C-343 in (a) Dry AOT RM, Urea Containing AOT RM, and Water Containing AOT RM and (b) Pure Solvents

(a) Reverse Micelle			
sample	w_0	λ_{abs}(max)/nm	λ_{em}(max)/nm
AOT RM	0	402	443
RM + urea 0.046 M	0.12	403	454
RM + urea 0.213 M	0.56	405	460
RM + urea 0.30 M	0.79	406	461
RM + water 0.046 M	0.12	403	443
RM + water 0.213 M	0.56	403	446
RM + water 0.30 M	0.79	404	448
RM + water 0.76 M	2.0	408	460
RM + water 1.89 M	5.0	409	478
RM + water 2.85 M	7.5	411	483
RM + water 3.80 M	10.0	412	484
water RM + urea 3 M	10.0	414	484
water RM + urea 5 M	10.0	414	484
(b) Pure Solvents			
solvents		λ_{abs}(max)/nm	λ_{em}(max)/nm
n-heptane		428	436
water		432	490
MeOH		435	488
EtOH		435	488
MeCN		436	462

setup from IBH Horiba Jobin Yvon (U.S.). The experimental setup for TCSPC was described in detail in our earlier publications.[32,33] Briefly, we used a 405 nm diode laser (IBH, U.K., NanoLED-405 L, with a λ_{max} = 402 nm) having a fwhm of 89 ps as a sample excitation source. The fluorescence signals were collected in magic angle using a MCP-PMT (Hamamatsu, Japan) detector. The collecting wavelengths were varied from 415 to 585 nm. For time-resolved anisotropy study, we have used a motorized polarizer on the emission side. The emission intensities at perpendicular and parallel polarizations were collected alternatively for 30 s. For typical anisotropy decay, the difference between the peak counts at parallel and perpendicular polarization was kept to 5000. The G factor of the setup was measured using variable orientation of the polarizer. The excitation polarizer remained fixed at the horizontal position. The emission polarizer repetitively changed its position from vertical (resulting decay I_{HV}) to horizontal (resulting decay I_{HH}) with a 30 s time duration for each. The analysis of lifetime and anisotropy data was done by IBH DAS6 analysis software. Both the lifetime as well as anisotropy decay profiles were fitted with a minimum number of exponential. The excellence of each fitting was judged by χ^2 values and the visual inspection of the residuals. The value of $\chi^2 \sim 1$ was considered as the best fits for the plots. Experimental error in TCSPC measurement is ±5%.

3. RESULTS AND DISCUSSION

3.1. Steady State Absorption Spectra. The steady state absorption spectra of C-343 in urea/water containing RMs are shown in Figure 1, and the results are summarized in Table 1. In this context, it is pertinent to mention that C-343 has very low solubility in *n*-heptane and because of low solubility it forms aggregates in nonpolar solvents like *n*-heptane.[34] The observed peak at ~402 nm is ascribed to the monomer, whereas the peak at ~428 nm reflects the aggregated state of C-343 in *n*-heptane (Figure 1).[34] The solubility of C-343 increases in the presence of 0.38 M AOT, and it displays an absorption maximum at 402 nm,

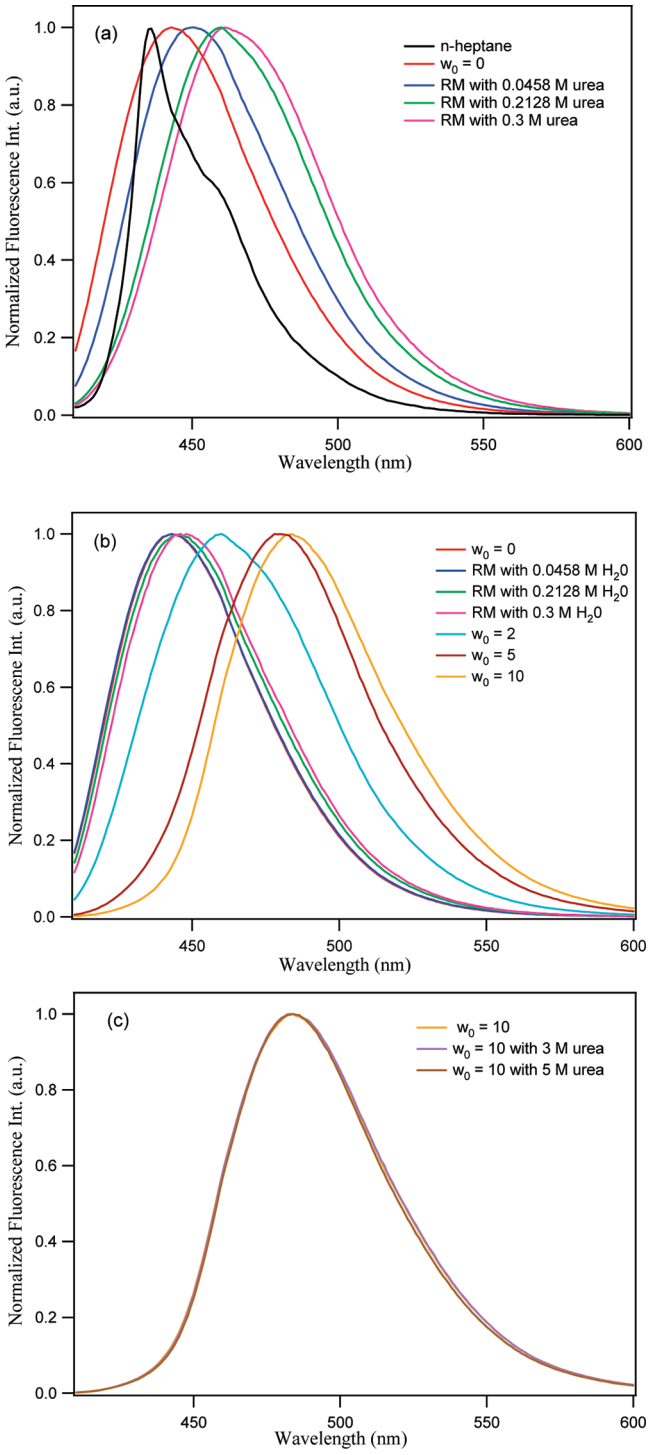

Figure 2. Steady state fluorescence emission spectra of C-343 (a) in *n*-heptane and different concentrations of urea in AOT RM, (b) at different concentrations of water in AOT RM, and (c) at w_0 = 10 and two different concentrations of urea in RM at w_0 = 10.

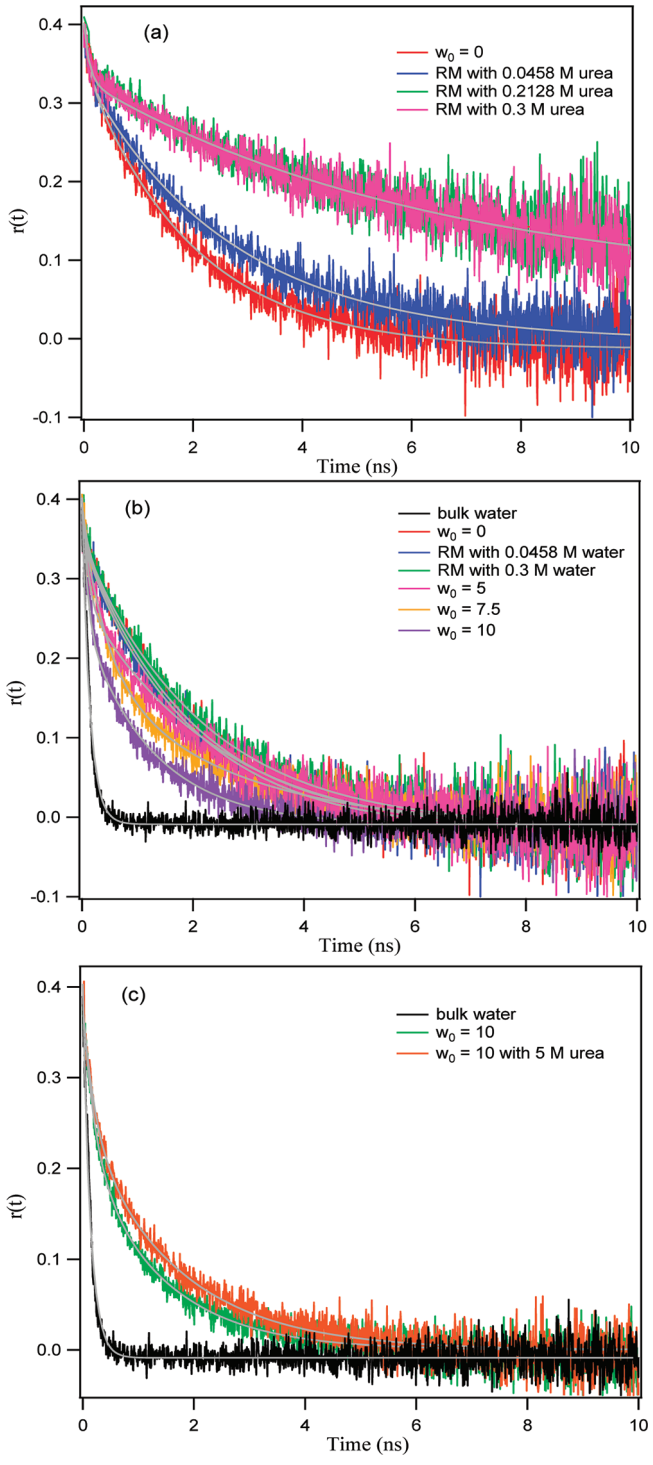

Figure 3. Fluorescence anisotropy decay profile of C-343 (a) at different concentrations of urea in RM, (b) at different concentrations of water in AOT RM and bulk water, and (c) at w_0 = 10 and two different concentrations of urea in RM at w_0 = 10 and bulk water.

which confirms that C-343 exists as a monomer in the presence of AOT. The monomer peak does not show any bathochromic shift in going from pure *n*-heptane to 0.38 M AOT. This is because the ground state of C-343 is less sensitive to polarity compared to the excited state.[34] On addition of urea to the 0.38 M AOT solution, a slight red shift is perceived (Table 1, Figure 1). However, the concentration of urea cannot go beyond 0.3 M due to the limited solubility of urea in the RM.[27,28] The slight red shift in absorption spectra indicates that the dye is experiencing slightly more polar milieu in the presence of urea inside the reverse micelle. For water RM, we extended our measurement until a water concentration of ∼3.8 M, corresponding to w_0 = 10. The absorption spectral features of C-343 in the *n*-heptane/AOT/water system are similar to that of literature reports.[29] It is notable that the absorption maximum of C-343 at w_0 = 10 is blue-shifted compared to bulk water (Table 1). This indicates that the environment sampled by the dye inside the RM differs from that of bulk water.

To verify the combined effect of urea and water on the absorption spectra, we have collected the same for C-343 at w_0 = 10 with various concentrations of urea dissolved in water. The results are shown in Figure 1c and tabulated in Table 1. The results clearly infer that absorption spectra of the dye display small red shift in the presence of urea in water RM compared to water RM alone. Recently, it has been reported that urea increases the bulk dielectric constant of the medium.[35] Hence, we ascribe the observed shift to the urea-induced increase in the local dielectric constant inside the reverse micelle.

3.2. Steady State Emission Spectra. The emission maximum of C-343 is monitored to characterize the environment experienced by the dye inside the reverse micelle, as the emission spectrum of the dye largely depends on the polarity of its surroundings.[34] The spectral features of C-343 in urea or (and) water containing RM are shown in Figure 2, and results are summarized in Table 1. The fluorescence emission maximum of C-343 in *n*-heptane appears at 436 nm. However, in the presence of 0.38 M AOT the spectrum displays a peak at ∼443 nm. On successive addition of urea, the emission peak is gradually red-shifted and there is almost ∼17 nm bathochromic shift while switching from dry to 0.3 M urea containing RM (Figure 2a and Table 1). The spectral shift indicates that the fluorescent dye is sensing more polar environment with the gradual addition of urea inside the RM. Interestingly, when the shift of emission spectra is compared to water RM, it suggests that the dye is more sensitive to urea compared to water; e.g., the emission maximum of C-343 in 0.3 M urea containing RM is located at 461 nm, whereas the same in 0.3 M water containing RM is situated at ∼448 nm (Figure 2b and Table 1). The comparison of the emission peaks of C-343 in various solvents suggests that the polarity of 0.3 M urea containing RM is close to acetonitrile (Table 1). The immense shift in emission spectra in the presence of urea offers a clear hint about the presence of "urea pool" inside the RM even at very low urea concentration (0.3 M). However, this is not the case for water RM, where "water pool" starts forming after w_0 = 2,[36] corresponding to a water concentration of 0.76 M. Moreover, C-343 exhibits an emission peak at 460 nm in 0.76 M water concentration of (w_0 = 2) inside the RM. Although the *n*-heptane/AOT/water system is well studied, in order to compare the results with urea RMs, we have extended our study up to w_0 = 10. The emission characteristics of C-343 in the *n*-heptane/AOT/water system are almost similar to that of literature report,[34] and as expected the emission peak is gradually red-shifted with respect to the water concentration of the RM. However, even at w_0 = 10, the peak maximum does not resemble that of bulk water. This infers that at this w_0 the dye molecule senses water environment, which is quite different from bulk water.

We have also monitored the emission spectra of C-343 in AOT RM at w_0 = 10 with increasing urea concentration in water

Table 2. Anisotropy Decay Characteristics of C-343 in Dry AOT RM, Urea Containing AOT RM, Water Containing AOT RM, and Urea−Water Mixture Containing RM

sample	w_0	r_0	a_{1r} (%)	τ_{1r} (ns)	a_{2r} (%)	τ_{2r} (ns)	a_{3r} (%)	τ_{3r} (ns)
AOT RM	0	0.40	10	0.100	90	1.97	–	–
RM + urea 0.046 M	0.12	0.39	12	0.090	88	2.64	–	–
RM + urea 0.213 M	0.56	0.38	13	0.060	24	1.60	63	8.4
RM + urea 0.30 M	0.79	0.37	14	0.065	23	1.76	63	9.2
RM + water 0.213 M	0.56	0.40	13	0.080	87	2.20	–	–
RM + water 0.30 M	0.79	0.40	13	0.090	87	2.17	–	–
RM + water 0.76 M	2.0	0.39	5	0.100	95	2.05	–	–
RM + water 1.89 M	5.0	0.38	34	0.445	66	2.92	–	–
RM + water 2.85 M	7.5	0.39	50	0.430	50	2.42	–	–
RM + water 3.80 M	10.0	0.38	47	0.260	53	1.54	–	–
water RM + urea 3 M	10.0	0.39	49	0.390	51	2.12	–	–
water RM + urea 5 M	10.0	0.37	35	0.220	65	1.68	–	–

to verify the combined effect of urea and water toward the emission spectra of C-343. However, we have noticed that the emission spectrum is almost unchanged with respect to urea concentration in water (Table 1 and Figure 2c). This suggests that the dye is sensing similar polarity of urea−water mixture as that of water alone inside the RM.

3.3. Time-Resolved Studies. *Time-Resolved Anisotropy.* Although steady state measurements provide a qualitative idea about the location of C-343 inside AOT-RM, to ascertain the location of the probe we have employed time-resolved fluorescence anisotropy study. Time-resolved fluorescence anisotropy is calculated using the following equation

$$r(t) = \frac{I_{||}(t) - GI_{\perp}(t)}{I_{||}(t) + 2GI_{\perp}(t)} \quad (1)$$

where $I_{||}(t)$ and $I_{\perp}(t)$ are fluorescence decays polarized parallel and perpendicular to the polarization of the excitation light, respectively. G is the correction factor for detector sensitivity to the polarization direction of the emission. These measurements provide information about the local viscosity as well as the rigidity of the milieu sensed by the dye and provide a notion about the location of the probe in the RM. The anisotropy decays are shown in Figure 3, and the results are tabulated in Table 2. The anisotropy decay of the dye in water can be well fitted by a single exponential decay function with a time constant of ∼130 ps (Figure 3). In contrast, the rotational time constants of the dye in the RM are a few orders larger in magnitude compared to bulk water. These results clearly suggest that the dye molecules are experiencing a more rigid milieu inside the RM than bulk water, irrespective of the nature/composition of loading solvents or molecules. Moreover, the anisotropy decay profiles of C-343 in water containing RM are nonexponential in nature, which is consistent with literature reports.[29]

The anisotropy results conspicuously indicate that the dye molecule is sensing a more hindered environment in urea containing RM compared to water containing RM (Table 2), even though the concentration of urea inside the RM is reasonably lower than in water. Recently, SANS studies of urea containing AOT RM revealed that urea molecules are encapsulated as small-sized ellipsoidal hydrogen-bonded clusters within the hydrophilic micellar core of the AOT RM.[28] This is also reflected in the anisotropy decay profile of the dye in urea containing RM, where we have noticed that the rotational motion of the dye is not at all completed within our observation time scale after the urea concentration of 0.046 M (Figure 3a), and this may be ascribed to the rigidity of the urea cluster around the dye molecule. Moreover, the anisotropy decay profiles clearly reveal that the environment of AOT-RM in the presence of urea is more hindered than that of dry AOT-RM. But this is not true for water RMs, where it has been observed that rotational motion of the probe becomes faster as the water content of the RM increases (Figure 3b, Table 2). This demonstrates that urea encapsulation to RM increases the rigidity of the environment inside the RM compared to dry as well as water RM due to the formation of molecular clusters by urea inside the RM.

At $w_0 = 0$, the dye molecules exclusively located at the micellar interface near the AOT head groups, as "water pool" does not exist at $w_0 = 0$. This is confirmed by the anisotropy decay profile of the dye, where the rotational motion of dye takes place on a 1.9 ns time scale. Previously, the rotational relaxation time for dry AOT RM has been shown via electron spin resonance (ESR) to be ∼1.2 ns.[36] As w_0 increases, a small rotational component is observed on the time scale of ∼200−445 ps along with the above-mentioned nanosecond component. Additionally, the magnitude of the picosecond component increases and the relative contribution of the nanosecond component decreases as w_0 increases. This observation infers that the dye molecules are experiencing a decreasingly restrictive milieu with increase in water content of the RM. Interestingly, even at $w_0 = 10$, the dye molecules do not sample a bulklike environment. The nanosecond component in rotational relaxation reflects the rotational motion of the dye molecules intercalated between the AOT head groups. On the other hand, the faster component of ∼260−445 ps might be ascribed to rotational relaxation of the C-343 residing in between interface and water pool, and the dye molecules find an average environment as the dye may diffuse toward the water pool during the excited state lifetime of the dye.

To check the effect of urea toward the rigidity of water structure, we have collected the anisotropy decay profiles of C-343 in AOT RM at a particular w_0 with varying urea concentration in water. We have observed that urea has almost negligible effect on the rotational motion of C-343 (Figure 3c). This means that rigidity of the surrounding environment of C-343 in water is not changing in the presence of urea. This is consistent with the observations that there are no major disruptions of the hydrogen

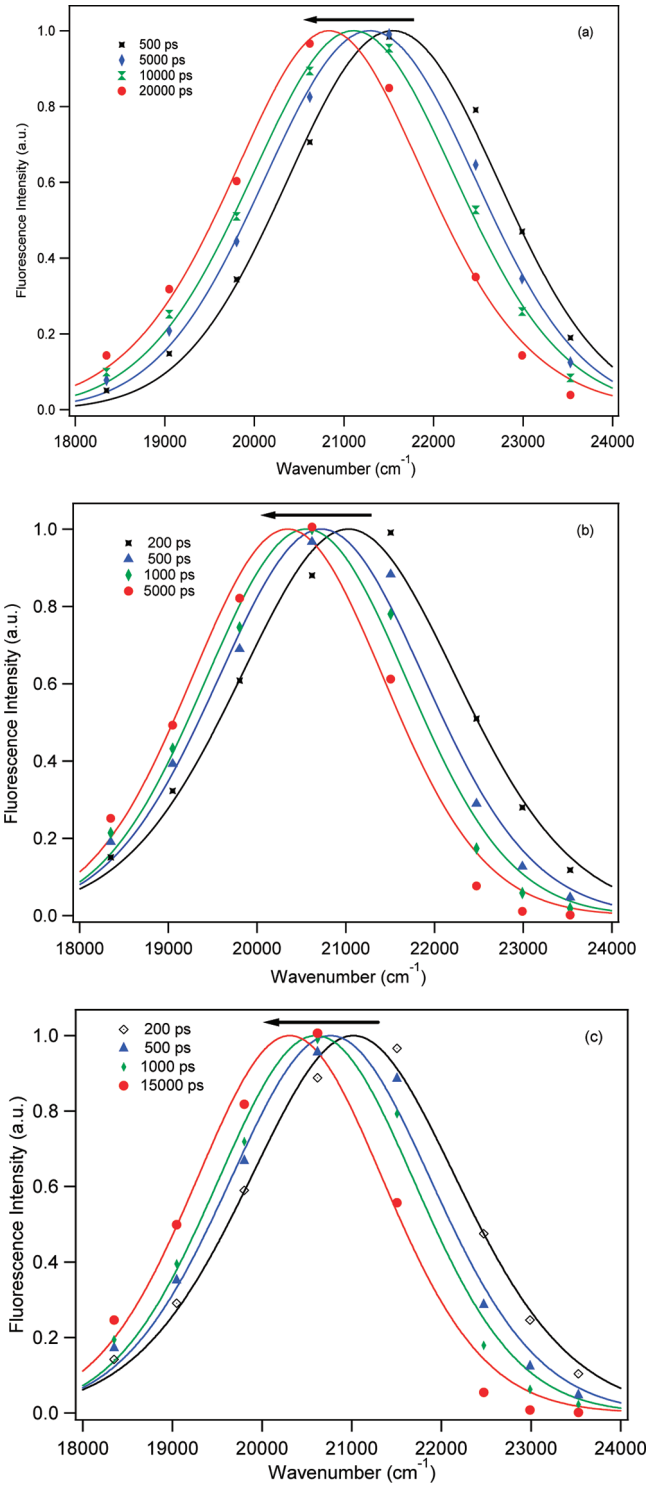

Figure 4. Time-resolved emission spectra (TRES) of C-343 (a) in 0.3 M urea containing RM, (b) at w_0 = 10, and (c) at 5 M urea containing RM at w_0 = 10.

bond network of water in the presence of urea.[20,37] The slight change in anisotropy decay might arise due to increased viscosity inside the RM by the addition of urea.

Although the dye molecules have negligible solubility in *n*-heptane, we cannot rule out the possibility of very few dye molecules residing in *n*-heptane. To get a quantitative idea of the dye partition between the *n*-heptane/water system, we have estimated the partition coefficient of the dye using UV−vis absorption spectroscopy. The partition coefficient for the *n*-heptane/water system is 0.06 (±0.01). This suggests that the solubility of C-343 in *n*-heptane is much less. The 60−100 ps component in anisotropy decay might reflect the rotational relaxation of the dye molecules situated in *n*-heptane (Table 2). Interestingly, this 100 ps component exists in dry urea and low-water containing RM. However, this dynamics is no longer observed in water or urea−water RM after a certain water concentration. This observation is tempting us to anticipate that the incorporation of water or urea−water mixture favors the transfer of more dye molecules from *n*-heptane to the reverse micelle. One possible reason may be the size of the RM, which increases with the addition of polar solvent. The larger size of the RM accommodates a higher number of dye molecules, and hence the dye molecules are no longer available in *n*-heptane at higher concentration of water or urea−water mixture of the RM.

Dynamic Fluorescence Stokes Shift. To probe the alteration of the dynamical properties of urea inside the reverse micelle, we have examined picosecond-resolved solvation dynamics of the dye (C-343) in AOT RM. For the purpose of comparison, the dynamic properties of water as well as urea−water mixture inside the RM have also been investigated using the same dye molecule. The fluorescence transients of C-343 in urea containing RM at different wavelengths ranging from 415 to 585 nm (10 nm successive intervals from 415 to 445 nm and consecutive 20 nm interval from 465 to 585 nm) have been collected, and it was found that the red end side of the transient displays prominent growth, indicating the dye molecule is gradually solvated with time. The fluorescence decays of C-343 at different wavelengths of other RMs, for example, water and urea−water containing RMs, have a similar type of features. In this context, it is relevant to mention that the decays at the short and long wavelengths of C-343 are identical in the pure solvents, e.g., *n*-heptane and water as well as in the urea−water mixture. The time-resolved emission spectra (TRES) have been constructed from the fluorescence decays at different wavelengths adopting the procedure given by Fleming and Maroncelli.[38] Representative TRES of C-343 in RM is shown in Figure 4. The solvent relaxation process immediately after photoexcitation of the probe is characterized by the solvation time correlation function $C(t)$, which is defined as

$$C(t) = \frac{\nu(t) - \nu(\infty)}{\nu(0) - \nu(\infty)} \tag{2}$$

where $\nu(0)$, $\nu(t)$, and $\nu(\infty)$ are the observed frequencies at time zero, t, and infinity, respectively. $\nu(t)$ is estimated from the log-normal fitting of the TRES at time t. Similarly, $\nu(\infty)$ is chosen from the log-normal fitting of the TRES at infinity time, when the frequency is almost unchanged. However, the time-zero fluorescence spectrum ($\nu(0)$) is estimated with the help of the method proposed by Fee and Maroncelli.[39] According to Fee and Maroncelli,[39] the $\nu(0)$ can be calculated by the following equation

$$\nu_{\mathrm{fl,p,md}}(t = 0) \approx \nu_{\mathrm{p,md}} - [\nu_{\mathrm{abs,np,md}} - \nu_{\mathrm{fl,p,md}}] \tag{3}$$

where the subscripts "p" and "np" refer to the polar and nonpolar spectra, respectively, and the frequencies here are not the values at the maxima but correspond to the midpoint frequencies

$$\nu_{\mathrm{md}} = (\nu_{-} + \nu_{+})/2 \tag{4}$$

Table 3. Calculated Time-Zero Fluorescence Maxima, Observed Time-Zero Fluorescence Maxima, and Missing Components

sample	$\nu_0{}^a{}_{(cal)}$ (cm^{-1})	$\nu_{0(obs)}$ (cm^{-1})	$\Delta\nu^b{}_{(cal)}$ (cm^{-1})	$\Delta\nu^c{}_{(obs)}$ (cm^{-1})	% MC[d]
RM	23864	22508	1903	547	71
RM + urea 0.046 M	23830	22054	2539	763	69
RM + urea 0.213 M	23781	21637	3221	1077	67
RM + urea 0.30 M	23732	21591	3213	1072	66
RM + water 0.046 M	23802	22517	1798	513	71
RM + water 0.213 M	23743	22462	2117	836	61
RM + water 0.30 M	23681	22404	2295	1018	56
w_0 = 2	23428	22161	2850	1583	45
w_0 = 5	23230	21850	2813	1433	49
w_0 = 10	23158	21638	2844	1324	53
w_0 = 10 + urea 3 M	23082	21509	2820	1247	56
w_0 = 10 + urea 5 M	23063	21427	2840	1204	58

[a] $\Delta\nu_{(cal)}$ determined using the Fee−Maroncelli method.[37] [b] $\Delta\nu_{(cal)} = \nu_{0(cal)} - \nu_\infty$. [c] $\Delta\nu_{(obs)} = \nu_{0(obs)} - \nu_\infty$. [d] MC: Missing component.

where ν_- and ν_+ are the low and high frequencies at the half-height points on the low and high frequency sides of the spectra. The maximum frequency at time zero, $\nu(0)$, is estimated as the sum of $\nu_{fl,p,md}(t = 0)$ and the difference between the midpoint and maximum frequencies in the steady state fluorescence spectrum of the same system (Table 3). The calculated $\nu(0)$ is used to construct $C(t)$. The decay properties of $C(t)$ are shown in Figure 5, and the results are tabulated in Table 4. Interestingly, the decay of $C(t)$ starts from a value lesser than unity (Figure 5). This is because the ultrafast dynamics in these systems cannot be captured by our TCSPC setup (<40 ps). Here, it should be mentioned that although the decays are not starting from unity, in order to make a comparison we have provided average solvation time based on the percentage of the dynamics detected by our setup (Table 4).

The solvation time τ_s is defined as follows according to the continuum theory[40]

$$\tau_s = \frac{2\varepsilon_\infty + \varepsilon_c}{2\varepsilon_0 + \varepsilon_c}\tau_D \qquad (5)$$

where ε_0 and ε_∞ are the static and high frequency dielectric constant of the solvent and τ_D is the dielectric relaxation time. ε_c is the dielectric constant of the cavity surrounding the probe.

In heterogeneous environment like RM, the interpretation of solvation dynamics results depends on the location of the probe, as the dye might have a distribution between nonpolar solvent and reverse micelle. As the monitoring dye (C-343) is anionic in nature (as the pK_a of C-343 is ~4.6[41]), almost all the dye molecules prefer to stay inside RM. The partition coefficient experiment in the *n*-heptane/water system (described in the Time-Resolved Anisotropy section) also indicates that the dye has very minimum solubility in *n*-heptane. Moreover, our steady state (absorption and fluorescence) as well as time-resolved fluorescence anisotropy results also suggest that most of dye molecules prefer to stay at the interface of the RM, whereas few dye molecules reside between the interface and "water pool". However, as we have already discussed in the Time-Resolved Anisotropy section, almost 10% of the dye molecules remain in the bulk *n*-heptane in the case of dry urea and low water containing RM due to the smaller sizes of these RMs.

It is conspicuous from Table 4 that the solvation dynamics of the dye is very slow for dry AOT RM and occurs on a ~14 ns time scale. The slow solvation time in dry RM might arise due to solvation by Na^+ ions, as it is already established that ionic solvation is quite slow.[42,43] The long lifetime of ~14 ns corresponds to ionic solvation. The fast component of ~200 ps is attributed to the presence of a trace amount of water in AOT, which is very difficult to remove. In literature, the solvation dynamics resulting in pure AOT RM is scarce. The only result that we are able to find out is that published by Sarkar et al. using Coumarin 152 as a solvation probe.[44] The reported solvation time by Sarkar et al. is ~12.22 ns in dry AOT-RM using C-152 as solvation probe.[44] However, we have observed a solvation time of ~14 ns in dry AOT RM. The relative difference in solvation time in our case and that of Sarkar et al. may turn up due to the use of a different type of solvation probe.

The results in Table 4 demonstrate that the solvation time of C-343 is escalating with the increase in urea concentration inside the AOT RM; e.g., the average time of solvation for C-343 in dry AOT RM is ~14 ns, whereas the same in 0.3 M urea containing RM is ~17 ns. However, the solvation time in RM containing 0.3 M water is very close to that of dry AOT RM (Figure 5a, Table 4). This is reasonable as the water pool of RM does not exist at this water concentration, and all the water molecules are likely to be located at the interface of AOT RM.[45] It is already perceived that the hydrodynamic radius of the water RM at $w_0 \leq 2$ is minuscule,[45] which suggests that this water concentration (0.3 M) has a trifling effect on the size and shape of the RM. On the other hand, 0.3 M urea has colossal influence on the size of AOT RM. SANS study indicates that the radius of quite spherical urea−AOT aggregate increases with urea and falls within the range of 15−25 Å,[27,28] which is equivalent to the variation of water pool size of RM from w_0 = 1 to w_0 = 6.[46] Moreover, SANS study infers that urea molecules are molecularly dispersed among the AOT hydrophilic head groups at lower concentration (<0.213 M), and at higher concentration they form molecular clusters surrounded by appropriately oriented AOT molecules.[27,28] These urea clusters are very rigid as they are strongly hydrogen bonded, and hence, their movements are extremely restricted. Therefore, the observed slow component (17 ns) in urea RM is attributed to the slow dynamics of urea clusters. The fast component (0.60−1.11 ns), with a negligible contribution of ~2−4%, might be attributed to the dynamics of waters and (or) urea molecules at the interfacial region of the RM. It would be interesting if we could be able to monitor the urea dynamics at

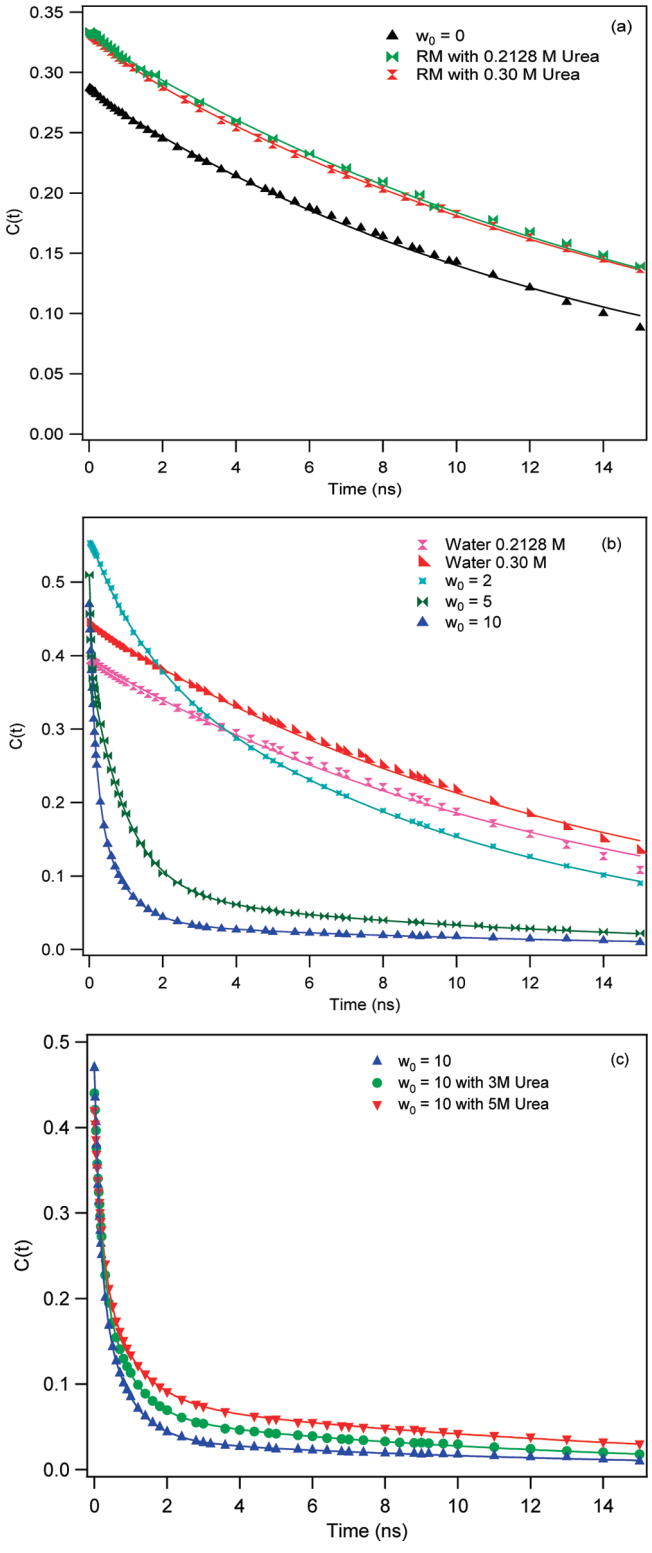

Figure 5. Decay of solvent correlation function ($C(t)$) of C-343 (a) in dry AOT and different urea containing RM, (b) in dry AOT and different water containing RM, and (c) at w_0 = 10 and two different concentrations of urea in RM at w_0 = 10.

higher concentration of urea, but due to the limited solubility of urea in AOT RM, we are unable to detect urea dynamics at higher urea concentrations (>0.3 M). It is noteworthy to mention here that formamide (FA) has a close structural resemblance to urea and also displays hindered solvation dynamics inside the reverse micelle, and the dynamics becomes faster as the FA concentration increases.[47,48] The solvation dynamics of FA inside the reverse micelle decreases from 9.45 to 6.2 ns with the increase in FA concentration,[47] whereas the same for urea increases from ~14.4 to ~17 ns as the concentration of urea inside the RM increases. The different solvation dynamics features between urea and FA arise due to different kinds of interactions inside the RM. The concentration dependence of FA dynamics inside the RM is attributed to the complex hydrogen bonding interactions between FA and AOT or FA and FA in the polar solvent pool of the RM.[47] For urea RMs, concentration dependence of solvation dynamics inside the RM is ascribed to the formation of molecular cluster at higher urea concentration (≥0.213 M).

The solvation dynamics of water inside AOT RM is nonexponential in nature after $w_0 \geq 2$ (Table 4, Figure 5a). The nonexponential feature of solvation dynamics signifies the existence of different kinds of water molecules inside the reverse micelle. Here, it is relevant to mention that FT-IR and ultrafast infrared studies revealed the existence of three diverse types of water molecules in the AOT RM, and they are termed as "bound water", "trapped water", and "free water".[46,49] Free water forms water cluster after a certain concentration, and this is designated as the water pool of the RM. Considering the FT-IR results, we anticipate that the triexponential feature of solvation dynamics reflects the dynamics of three distinct kinds of water inside the reverse micelle. The fast component of solvation dynamics (120−160 ps) might reflect the dynamics of water cluster in the water pool of the RM (Table 4). This suggests that the dynamics of the water cluster is much faster than that of the urea cluster, which implies that water clusters inside the reverse micelle are not rigid like urea cluster. The slower component of ~1.00 ns might be attributed to the trapped water molecules in between neighboring surfactant head groups, and the slowest component (~11.5−12.2 ns) might be ascribed to the dynamics of bound water molecules, those that are strongly hydrogen bonded to the wall of the RM through the Na^+ ions.[44] Surprisingly, at w_0 = 2, the solvation dynamics consists of only two components having solvation time of 1.28 and ~9 ns (Table 3). In analogy to our prophecies about solvation dynamics components at higher w_0, we believe that 1.28 and ~9 ns components are featured by the trapped and bound water molecules, respectively. This insinuates that the solvation dynamics of C-343 at w_0 = 2 is devoid of the free water dynamics, which alludes to the nonexistence of a water pool at w_0 = 2. This conjecture is supported by the literature, where it has been reported that at this w_0 essentially all the water molecules are associated with sulfonate head groups of AOT.[49] Unless noted otherwise, the dynamics of water pool water is almost 100 times slower than that of bulk water as the relaxation dynamics of bulk water around C-343 takes place on a <1 ps time scale.[29] It is believed that chemical exchange between interfacial water (trapped and bound water) and the water pool water would result in apparently more sluggish solvation time of water pool water than that of bulk water.[50]

Here, it is worth mentioning that most of the previous studies have detected only two kinds of water dynamics inside the AOT RM.[44,51] However, in this study we have seen three different dynamics corresponding to three different types of water molecules inside the reverse micelle. Riter et al. also reported the dynamics of three different kinds of water molecules based on the ultrafast components of C-343 in AOT RM.[29] Although we have

Table 4. Decay Characteristics of Solvent Correlation Function ($C(t)$) of C-343 in AOT-RM, Urea Containing AOT-RM, and Water Containing AOT-RM

sample	w_0	a_1 (%)	τ_1 (ns)	a_2 (%)	τ_2 (ns)	a_3 (%)	τ_3 (ns)	$\langle\tau_{av}\rangle^a$ (ns)
RM	0	2.0	0.20	98.0	14.12	–	–	13.84
RM + urea 0.046 M	0.12	1.0	0.20	99.0	14.55	–	–	14.40
RM + urea 0.213 M	0.56	2.0	0.60	98.0	17.16	–	–	16.83
RM + urea 0.30 M	0.79	4.0	1.11	96.0	17.52	–	–	16.86
RM + water 0.213 M	0.56	1.0	0.40	99.0	13.80	–	–	13.67
RM + Water 0.30 M	0.79	1.8	0.40	98.2	13.75	–	–	13.51
RM + water 0.76 M	2.0	22	1.28	78.0	9.32	–	–	7.55
RM + water 1.89 M	5.0	22	0.12	63.0	1.00	15	11.52	2.38
RM + water 3.80 M	10.0	51	0.16	40.0	0.74	09	12.16	1.47
water RM + urea 3M	10.0	45	0.19	40.0	0.82	15	12.00	2.21
water RM + urea 5M	10.0	42	0.20	38.0	0.90	20	13.70	3.16

[a] $\langle\tau_{av}\rangle = a_1\tau_1 + a_2\tau_2 + a_3\tau_3$.

missed such ultrafast components in our study due to our limited instrument resolution (IRF ~ 80 ps), still the dynamics of all the three kinds of water molecules inside the reverse micelle are efficiently detected. The use of a highly water-soluble solvation probe like C-343 might be the apparent reason for effective detection of three distinct kinds of water dynamics inside the RM. In the case of C-343 in RM, the majority of the dye molecules reside at the interface of the micelle. However, a fraction of dye molecules also dwell in between the interface and water pool, and there is a finite probability that during the excited state lifetime dye molecules may diffuse toward the water pool of the RM. Therefore, C-343 molecules can probe the dynamics of three different kinds of water molecules present inside the RM. The biexponential feature of solvation dynamics reported by other groups results from the use of neutral solvation probe, the solubility of which in water is very low.[44,51] Hence, the probability of finding this neutral solvation probe in the water pool of the RM is much less; instead they subsist at the interface of the RM. Although it has been reported that the nanosecond component of solvation dynamics corresponds to free water in the water pool of the RM,[44,51] we believe that the nanosecond component does not reflect the dynamics of free water of the RM; rather, it displays the dynamics of the trapped water inside the reverse micelle. This can be justified from the fact that free water in the water pool of the RM generally comprises a dynamics of 120–160 ps (Table 4). These observations lead us to conclude that heterogeneity of water environment could be detected by the solvation dynamics technique with the help of proper choice of solvation probe.

We have also monitored the dynamics of urea–water mixtures inside the AOT RM with increasing urea concentration to get insight about the effect of urea on the overall solvation dynamics feature. The characteristics of the solvation dynamics feature are shown in Figure 5b, and the results are tabulated in Table 4. It is unequivocal from the results that solvation dynamics is slowing down with increasing urea concentration in water RM. Small angle X-ray scattering (SAXS) study indicates that urea cannot modify the RM structure with respect to its shape and size.[52] Hence, the observed slow solvation dynamics is not arising due to the size of the RM. The dielectric spectroscopic study of urea–water liquid structure proposed that there are two types of hydrated water molecules in urea solution, which are strongly and weakly associated to the urea molecule.[53] Moreover, polarization-resolved pump–probe spectroscopy elucidated the effect of urea on the structure and dynamics of water.[20] It was found that a small fraction of the water molecules are strongly associated with urea and those water molecules flaunt an orientational dynamics that are more than six times slower than in bulk water.[20] Therefore, the observed slow dynamics in the presence of urea might be attributed to the dynamics of those strongly associated water molecules with urea. This is also reflected in our solvation dynamics results, where it is seen that the time constant as well as amplitude of the slow component is increasing on going from water RM to urea–water containing RM. However, we cannot rule out the possibility that the observed slow dynamics might reflect the dynamics of a few urea molecules, those that are strongly hydrogen bonded with surroundings urea and (or) water molecules.

We have already mentioned that in our experimental setup we miss ultrafast components of solvation dynamics due to limited instrumental resolution, and we have estimated the missing component with the help of the procedure developed by Fee and Maroncelli.[39] It is noticeable that dry urea and lower water content RMs have a larger percentage of missing component than a higher concentration of water as well as urea–water containing RMs (Table 3). This is probably due to the fact that in these systems a small percentage of dye molecules (~10%) reside outside the reverse micelle, and they are also excited along with the dye molecules staying inside the reverse micelle. The solvation dynamics of the dye molecules, those residing outside the reverse micelle, might be taking place on several a picosecond time scale. Therefore, the overall solvation component detected in these systems is significantly lower than other water and urea–water containing RMs. The missing component trend in the case of water RMs shows a good agreement with the previous report.[54] According to Fee and Maroncelli, if the absorption spectrum of the dye in nonpolar solvent is not structureless, the reliability of the missing component is questionable.[39] In our case, as the absorption spectra of the dye in nonpolar solvent is structured, the calculated missing component may not be precise.

4. CONCLUSION

In this work, we have observed that C-343 in 0.3 M urea containing RM exhibits a huge bathochromic shift in emission spectra compared to 0.3 M water containing RM. Comparing the

peak maximum of C-343 in pure solvents, it is found that 0.3 M urea in RM produces a polarity, which is closer to acetonitrile. The dynamics of urea in the RM has been also monitored using the time-resolved Stokes shift method. It has been observed that after a certain concentration, urea exhibits highly retarded dynamics compared to dry as well as water RM, and this is ascribed to the highly hydrogen-bonded network of urea molecules inside the reverse micelle. Time-resolved anisotropy study also supports the existence of highly networked urea cluster inside the reverse micelle. Moreover, to get an idea about the perturbation of urea on the overall solvation dynamics feature, we have also probed the dynamics of urea−water mixtures inside the AOT RM with increasing urea concentration. It has been observed that with the increase in urea concentration, the overall dynamics becomes slower, and it might be attributed to the presence of a few water or urea molecules, those that are strongly associated with surroundings urea and (or) water by hydrogen bonds.

AUTHOR INFORMATION

Corresponding Author

*E-mail p.hazra@iiserpune.ac.in; tel. +91-20-2590-8077; fax +91-20-2589 9790.

ACKNOWLEDGMENT

We express gratitude to Prof. K. N. Ganesh, Director, IISER-Pune, for providing excellent research facilities. This work is partly supported by SERC, Department of Science and Technology (DST), Government of India. We are thankful to the anonymous reviewers for their meticulous inspection of the manuscript and constructive suggestions.

REFERENCES

(1) Yamazaki, T.; Kovalenko, A.; Murashov, V. V.; Patey, G. N. *J. Phys. Chem. B* **2010**, *114*, 613–619.
(2) Das, A.; Mukhopadhyay, C. *J. Phys. Chem. B* **2009**, *113*, 12816–12824.
(3) Stumpe, M. C.; Grubmüller, H. *J. Phys. Chem. B* **2007**, *111*, 6220–6228.
(4) Lee, M. E.; van der Vegt, N. F. A. *J. Am. Chem. Soc.* **2006**, *128*, 4948–4949.
(5) van der Vegt, N. F. A.; Trzesniak, D.; Kasumaj, B.; van Gunsteren, W. F. *Chem. Phys. Chem.* **2004**, *5*, 144–147.
(6) Trzesniak, D.; van der Vegt, N. F. A.; van Gunsteren, W. F. *Phys. Chem. Chem. Phys.* **2004**, *6*, 697–702.
(7) Wallqvist, A.; Covell, D. G. *J. Am. Chem. Soc.* **1998**, *120*, 427–428.
(8) Ikeguchi, M.; Nakamura, S.; Shimizu, K. *J. Am. Chem. Soc.* **2001**, *123*, 677–682.
(9) Tobi, D.; Elber, R.; Thirumalai, D. *Biopolymers* **2003**, *68*, 359–369.
(10) Graziano, G. *J. Phys. Chem. B* **2001**, *105*, 2632–2637.
(11) Finer, E. G.; Franks, F.; Tait, M. J. *J. Am. Chem. Soc.* **1972**, *94*, 4424–4429.
(12) Turrell, G.; Hoccart, X. *J. Chem. Phys.* **1993**, *99*, 8498–8503.
(13) Vanzi, F.; Madan, B.; Sharp, K. *J. Am. Chem. Soc.* **1998**, *120*, 10748–10753.
(14) Chitra, R.; Smith, P. E. *J. Phys. Chem. B* **2000**, *104*, 5854–5864.
(15) Bennion, B. J.; Daggett, V. *Proc. Natl. Acad. Sci. U.S.A* **2003**, *100*, 5142–5147.
(16) Caflisch, A.; Karplus, M. *Structure* **1999**, *7*, 477–488.
(17) Kaatze, U.; Gerke, H.; Pottel, R. *J. Phys. Chem.* **1986**, *90*, 5464–5469.
(18) Idrissi, A.; Bartolini, P.; Ricci, M.; Righini, R. *J. Chem. Phys.* **2001**, *114*, 6774–6780.
(19) Shimizu, A.; Fumino, K.; Yukiyasu, K.; Taniguchi, Y. *J. Mol. Liq.* **2000**, *85*, 269–278.
(20) Rezus, Y. L. A.; Bakker, H. J. *Proc. Natl. Acad. Sci. U.S.A* **2006**, *103*, 18417–18420.
(21) Idrissi, A.; Sokolić, F.; Perera, A. *J. Chem. Phys.* **2000**, *112*, 9479–9488.
(22) Tsai, J.; Gerstein, M.; Levitt, M. *J. Chem. Phys.* **1996**, *104*, 9417–9430.
(23) Reimers, J. R.; Watts, R. O.; Klein, M. L. *Chem. Phys.* **1982**, *64*, 95–114.
(24) Gosting, L. J.; Akeley, D. F. *J. Am. Chem. Soc.* **1952**, *74*, 2058–2060.
(25) Lin, Z.; Wang, Z.; Chen, C.; Lee, M.-H. *J. Chem. Phys.* **2003**, *118*, 2349–2356.
(26) Wu, K.; Lin, S.; Chen, C. *Opt. Mater.* **1993**, *2*, 185–189.
(27) Calvaruso, G.; Minore, A.; Liveri, V. T. *J. Colloid Interface Sci.* **2001**, *243*, 227–232.
(28) Caponetti, E.; Chillura-M, D.; Ferrante, F.; Pedone, L.; Ruggirello, A.; Liveri, V. T. *Langmuir* **2003**, *19*, 4913–4922.
(29) Riter, R. E.; Willard, D. M.; Levinger, N. E. *J. Phys. Chem. B* **1998**, *102*, 2705–2714.
(30) Willard, D. M.; Riter, R. E.; Levinger, N. E. *J. Am. Chem. Soc.* **1998**, *120*, 4151–4160.
(31) Shirota, H.; Horie, K. *J. Phys. Chem. B* **1999**, *103*, 1437–1443.
(32) Sengupta, A.; Hazra, P. *Chem. Phys. Lett.* **2010**, *501*, 33–38.
(33) Sengupta, A.; Khade, R. V.; Hazra, P. *J. Photochem. Photobiol., A* **2011**, *221*, 105–112.
(34) Correa, N. M.; Levinger, N. E. *J. Phys. Chem. B* **2006**, *110*, 13050–13061.
(35) Dias, L. G.; Florenzano, F. H.; Reed, W. F.; Baptista, M. S.; Souza, S. M. B.; Alvarez, E. B.; Chaimovich, H.; Cuccovia, I. M.; Amaral, C. L. C.; Brasil, C. R.; Romsted, L. S.; Politi, M. J. *Langmuir* **2002**, *18*, 319–324.
(36) Krishnakumar, S.; Somasundaran, P. *J. Colloid Interface Sci.* **1994**, *162*, 425–430.
(37) Panuszko, A.; Bruzdziak, P.; Zielkiewicz, J.; Wyrzykowski, D.; Stangret, J. *J. Phys. Chem. B* **2009**, *113*, 14797–14809.
(38) Maroncelli, M.; Fleming, G. R. *J. Chem. Phys.* **1987**, *86*, 6221–6239.
(39) Fee, R. S.; Maroncelli, M. *Chem. Phys.* **1994**, *183*, 235–247.
(40) Van der Zwan, G.; Hynes, J. T. *J. Phys. Chem.* **1985**, *89*, 4181–4188.
(41) Riter, R. E.; Undiks, E. P.; Levinger, N. E. *J. Am. Chem. Soc.* **1998**, *120*, 6062–6067.
(42) Bart, E.; Huppert, D. *Chem. Phys. Lett.* **1992**, *195*, 37–44.
(43) Chapman, C. F.; Maroncelli, M. *J. Phys. Chem.* **1991**, *95*, 9095–9114.
(44) Hazra, P.; Chakrabarty, D.; Sarkar, N. *Langmuir* **2002**, *18*, 7872–7879.
(45) Maitra, A. *J. Phys. Chem.* **1984**, *88*, 5122–5125.
(46) Jain, T. K.; Varshney, M.; Maitra, A. *J. Phys. Chem.* **1989**, *93*, 7409–7416.
(47) Shirota, H.; Segawa, H. *Langmuir* **2004**, *20*, 329–335.
(48) Riter, R. E.; Undiks, E. P.; Kimmel, J. R.; Levinger, N. E. *J. Phys. Chem. B* **1998**, *102*, 7931–7938.
(49) Moilanen, D. E.; Levinger, N. E.; Spry, D. B.; Fayer, M. D. *J. Am. Chem. Soc.* **2007**, *129*, 14311–14318.
(50) Bagchi, B. *Chem. Rev.* **2005**, *105*, 3197–3219.
(51) Sarkar, N.; Das, K.; Datta, A.; Das, S.; Bhattacharyya, K. *J. Phys. Chem.* **1996**, *100*, 10523–10527.
(52) Itri, R.; Amaral, C. L. C.; Politi, M. J. *J. Chem. Phys.* **1999**, *111*, 7668–7674.
(53) Hayashi, Y.; Katsumoto, Y.; Omori, S.; Kishii, N.; Yasuda, A. *J. Phys. Chem. B* **2007**, *111*, 1076–1080.
(54) Hazra, P.; Chakrabarty, D.; Sarkar, N. *Chem. Phys. Lett.* **2003**, *371*, 553–562.